cultured for 5 days in 1.35 mM deoxyguanosine (Sigma) using 0.05% trypsin (GIBCO) and 0.02% EDTA. Reaggregates were formed by mixing together the desired TSC and thymocytes at a 1:1 cell ratio (absolute number, 5×10^5 of each cell type) or TSC, thymocytes and dendritic cells at a cell ratio of 10:10:1 (absolute number of dendritic cells, 5×10^4). After pelleting the cells by centrifugation, the cell mixture was placed as a standing drop on the upper membrane surface of a Transwell culture well containing RPMI-1640 supplemented by 10% FCS and cultured for 72 h at 37 °C. In some experiments purified mouse IgG2b (20 μg ml^{-1}) (Pharmingen) or anti-Notch-1 monoclonal antibodies (20 μg ml^{-1}) was incubated with $CD69^{hi}$ thymocytes, TSC and dendritic cells for 30 min at 4 °C before reaggregate culture, then cell mixtures were cultured in the presence of the same antibody. All results shown were repeated 2–8 times with similar findings.

Preparation of dendritic cells

Dendritic cells were purified from spleen cells from C57BL/6 or B10.BR mice as described[29]. Briefly, low-density spleen cells recovered from a BSA gradient were incubated for 30 min with anti-CD4, anti-CD8 and anti-B220 monoclonal antibodies (Pharmingen). After incubation with this antibody cocktail, the cells were washed and antibody-coated cells were removed by sheep-anti-rat IgG-coupled magnetic beads (Dynabeads, Dynal). The resultant population contained 80–85% CD11c+ cells and is referred to as dendritic cells (DC) in this study.

Retroviral constructs and retroviral transfection

The retroviral vector encoding GFP (GFP–RV)[30] was provided by K. Murphy (Washington Univ., St. Louis). Mouse Notch-1 (+64–+1164) was amplified using Pfu DNA polymerase (Stratagene) and cloned into *Xho*I digested GFP–RV vector. The nucleotide sequence and orientation of the insert were confirmed by dideoxy sequencing. The Phoenix-Eco packaging cell line (gift from G. Nolan, Stanford) was transfected according to Nolan's protocol. Day 14 fetal thymocytes (5×10^6 ml^{-1}) from C57BL/6 or AND mice were infected using 1:1 volume of viral supernatant, polybrene (Sigma) at 8 μg ml^{-1} and mouse IL-7 (20 ng ml^{-1}) (Pharmingen), centrifuged at 1,800*g* for 45 min at room temperature, and incubated at 37 °C for 48 h. The GFP^+ cells purified by fluorescence-activated cell sorting were transferred into deoxyguanosine (1.35 mM; Sigma)-treated (5 days) day 14 fetal thymi from $MHC^{-/-}$ mice in the wells of a Terasaki plate (Applied Scientific). After 1 day, the repopulated thymus lobes were then cultured at 37 °C on the upper membrane surface of a Transwell culture well containing RPMI-1640 supplemented with 10% FCS. After 7 days culture, total cells were stained with Cychrome-conjugated anti-CD4 and PE-conjugated anti-CD8 monoclonal antibodies, then $CD4^+CD8^+$ cells were purified by electronic sorting. These $CD4^+CD8^+$ cells were reaggregated with TSC from C57BL/6 mice and cultured for 72 h. In the case of thymocytes from AND mice, total cells recovered after 7 days culture in repopulated thymic lobes were stimulated with Mu-DC and $CD4^+CD8^+CD69^+$ cells were purified by electronic sorting, which were reaggregated with TSC from C57BL/6 mice and cultured for 60 h.

Received 23 September 1999; accepted 31 January 2000.

1. Robey, E. & Fowlkes, B. J. Selective events in T cell development. *Annu. Rev. Immunol.* **12,** 675–705 (1994).
2. Davis, M. M. & Bjorkman, P. J. T-cell antigen receptor genes and T-cell recognition. *Nature* **334,** 395–402 (1988).
3. von Boehmer, H. CD4/CD8 lineage commitment: back to instruction? *J. Exp. Med.* **183,** 713–715 (1996).
4. Chan, S., Correia-Neves, M., Benoist, C. & Mathis, D. CD4/CD8 lineage commitment: matching fate with competence. *Immunol. Rev.* **165,** 195–207 (1998).
5. Robey, E. *et al.* An activated form of Notch influences the choice between CD4 and CD8 T cell lineages. *Cell* **87,** 483–492 (1996).
6. Deftos, M. L., He, Y. W., Ojala, E. W. & Bevan, M. J. Correlating notch signaling with thymocyte maturation. *Immunity* **9,** 777–786 (1998).
7. Kaye, J. *et al.* Selective development of CD4+ T cells in transgenic mice expressing a class II MHC-restricted antigen receptor. *Nature* **341,** 746–749 (1989).
8. Konig, R., Huang, L. Y. & Germain, R. N. MHC class II interaction with CD4 mediated by a region analogous to the MHC class I binding site for CD8. *Nature* **356,** 796–798 (1992).
9. Riberdy, J. M., Mostaghel, E. & Doyle, C. Disruption of the CD4-major histocompatibility complex class II interaction blocks the development of CD4(+) T cells *in vivo*. *Proc. Natl Acad. Sci. USA* **95,** 4493–4498 (1998).
10. Anderson, G., Jenkinson, E. J., Moore, N. C. & Owen, J. J. MHC class II-positive epithelium and mesenchyme cells are both required for T-cell development in the thymus. *Nature* **362,** 70–73 (1993).
11. Lucas, B. & Germain, R. N. Unexpectedly complex regulation of CD4/CD8 coreceptor expression supports a revised model for CD4+CD8+ thymocyte differentiation. *Immunity* **5,** 461–477 (1996).
12. Davis, C. B., Killeen, N., Crooks, M. E., Raulet, D. & Littman, D. R. Evidence for a stochastic mechanism in the differentiation of mature subsets of T lymphocytes. *Cell* **73,** 237–247 (1993).
13. Veillette, A., Zuniga-Pflucker, J. C., Bolen, J. B. & Kruisbeek, A. M. Engagement of CD4 and CD8 expressed on immature thymocytes induces activation of intracellular tyrosine phosphorylation pathways. *J. Exp. Med.* **170,** 1671–1680 (1989).
14. Wiest, D. L. *et al.* Regulation of T cell receptor expression in immature CD4+CD8+ thymocytes by p56lck tyrosine kinase: basis for differential signaling by CD4 and CD8 in immature thymocytes expressing both coreceptor molecules. *J. Exp. Med.* **178,** 1701–1712 (1993).
15. Kisielow, P., Bluthmann, H., Staerz, U. D., Steinmetz, M. & von Boehmer, H. Tolerance in T-cell-receptor transgenic mice involves deletion of nonmature CD4+8+ thymocytes. *Nature* **333,** 742–746 (1988).
16. Hogquist, K. A., Jameson, S. C. & Bevan, M. J. Strong agonist ligands for the T cell receptor do not mediate positive selection of functional CD8+ T cells. *Immunity* **3,** 79–86 (1995).
17. Teh, H. S. *et al.* Thymic major histocompatibility complex antigens and the alpha beta T- cell receptor determine the CD4/CD8 phenotype of T cells. *Nature* **335,** 229–233 (1988).
18. Basson, M. A., Bommhardt, U., Cole, M. S., Tso, J. Y. & Zamoyska, R. CD3 ligation on immature thymocytes generates antagonist-like signals appropriate for CD8 lineage commitment, independently of T cell receptor specificity. *J. Exp. Med.* **187,** 1249–1260 (1998).
19. Merkenschlager, M. *et al.* How many thymocytes audition for selection? *J. Exp. Med.* **186,** 1149–1158 (1997).
20. Iwata, M., Kuwata, T., Mukai, M., Tozawa, Y. & Yokoyama, M. Differential induction of helper and killer T cells from isolated CD4+CD8+ thymocytes in suspension culture. *Eur. J. Immunol.* **26,** 2081–2086 (1996).
21. Grakoui, A. *et al.* The immunological synapse: a molecular machine controlling T cell activation. *Science* **285,** 221–227 (1999).
22. Radtke, F. *et al.* Deficient T cell fate specification in mice with an induced inactivation of Notch1. *Immunity* **10,** 547–558 (1999).
23. Marshall, C. J. Specificity of receptor tyrosine kinase signaling: transient versus sustained extracellular signal-regulated kinase activation. *Cell* **80,** 179–185 (1995).
24. Matechak, E. O., Killeen, N., Hedrick, S. M. & Fowlkes, B. J. MHC class II-specific T cells can develop in the CD8 lineage when CD4 is absent. *Immunity* **4,** 337–347 (1996).
25. Sharp, L. L., Schwarz, D. A., Bott, C. M., Marshall, C. J. & Hedrick, S. M. The influence of the MAPK pathway on T cell lineage commitment. *Immunity* **7,** 609–618 (1997).
26. Bommhardt, U., Basson, M. A., Krummrei, U. & Zamoyska, R. Activation of the extracellular signal-related kinase/mitogen-activated protein kinase pathway discriminates CD4 versus CD8 lineage commitment in the thymus. *J. Immunol.* **163,** 715–722 (1999).
27. Felli, M. P. *et al.* Expression pattern of notch1, 2 and 3 and jagged1 and 2 in lymphoid and stromal thymus components: distinct ligand-receptor interactions in intrathymic T cell development. *Intl Immunol.* **11,** 1017–1025 (1999).
28. Beatus, P., Lundkvist, J., Oberg, C. & Lendahl, U. The notch 3 intracellular domain represses notch 1-mediated activation through Hairy/Enhancer of split (HES) promoters. *Development* **126,** 3925–3935 (1999).
29. Inaba, M. *et al.* Distinct mechanisms of neonatal tolerance induced by dendritic cells and thymic B cells. *J. Exp. Med.* **173,** 549–559 (1991).
30. Ouyang, W. *et al.* Inhibition of Th1 development mediated by GATA-3 through an IL-4- independent mechanism. *Immunity* **9,** 745–755 (1998).

Acknowledgements

This work was partially support by grants from the Illinois Department of Public Health and from NIH to L.M. and American Cancer Society and the Arthritis Foundation to C.D. K.Y. was supported in part by a fellowship from the Japan Society for the Promotion of Science. We thank B.J. Fowlkes and R. H. Schwartz for their helpful comments on this manuscript, J. Delon for insightful suggestions concerning data interpretation, and M. Verma for generating the antisense Notch-1 construct.

Correspondence and requests for materials should be addressed to R.N.G. (e-mail: Ronald_Germain@nih.gov).

DNA repair protein Ku80 suppresses chromosomal aberrations and malignant transformation

Michael J. Difilippantonio*, Jie Zhu†, Hua Tang Chen†, Eric Meffre‡, Michel C. Nussenzweig‡, Edward E. Max§, Thomas Ried* & André Nussenzweig†

** Genetics Department, National Cancer Institute, National Institutes of Health, Bethesda, Maryland 20892, USA*
† Experimental Immunology Branch, National Cancer Institute, National Institutes of Health, Bethesda, Maryland 20892, USA
‡ Laboratory of Molecular Immunology, and Howard Hughes Medical Institute, The Rockefeller Institute, New York, New York 10021, USA
§ Laboratory of Cell Regulation, Center for Biologics Evaluation and Research, Food and Drug Administration, National Institutes of Health, Bethesda, Maryland 20892, USA

Cancer susceptibility genes have been classified into two groups: gatekeepers and caretakers[1]. Gatekeepers are genes that control cell proliferation and death, whereas caretakers are DNA repair genes whose inactivation leads to genetic instability. Abrogation of both caretaker and gatekeeper function markedly increases cancer susceptibility. Although the importance of Ku80 in DNA double-strand break repair is well established, neither Ku80 nor other components of the non-homologous end-joining pathway

are known to have a caretaker role in maintaining genomic stability. Here we show that mouse cells deficient for *Ku80* display a marked increase in chromosomal aberrations, including breakage, translocations and aneuploidy. Despite the observed chromosome instabilities, *Ku80*$^{-/-}$ mice have only a slightly earlier onset of cancer[2,3]. Loss of p53 synergizes with Ku80 to promote tumorigenesis such that all *Ku80*$^{-/-}$*p53*$^{-/-}$ mice succumb to disseminated pro-B-cell lymphoma before three months of age. Tumours result from a specific set of chromosomal translocations and gene amplifications involving IgH and c-Myc, reminiscent of Burkitt's lymphoma. We conclude that *Ku80* is a caretaker gene that maintains the integrity of the genome by a mechanism involving the suppression of chromosomal rearrangements.

The three subunits of the DNA-dependent protein kinase, Ku70, Ku80 and DNA-PKcs, are, together with XRCC4 and Ligase IV, essential for the non-homologous end-joining (NHEJ) pathway in mammalian cells. Mice that carry the targeted disruption of components of the NHEJ pathway share some common phenotypic features including arrested lymphocyte development and increased sensitivity to ionizing radiation[3–9]. Deficiencies in Ku80, Ku70, XRCC4 and Ligase IV, but not in DNA-PKcs, result in growth retardation and decreased proliferation *in vitro*. This senescence has been proposed to result from an inability to repair double-strand breaks (DSBs) in DNA incurred during normal DNA metabolism[3].

p53 monitors chromosome damage and either arrests cell-cycle progression or triggers apoptosis in cells with unrepaired lesions[10]. To determine whether p53 is involved in the growth arrest of *Ku80*$^{-/-}$ mice and mouse embryo fibroblasts (MEFs), we generated *Ku80*$^{-/-}$*p53*$^{-/-}$ double-mutant mice. The absence of *p53* did not markedly affect the initial viability of *Ku80*$^{-/-}$*p53*$^{-/-}$ mice, and they were indistinguishable in size from *Ku80*$^{-/-}$ littermates. By contrast, inactivation of *p53* did alleviate the growth arrest of the *Ku80* knock-out MEFs (Fig. 1a, b). *Ku80*$^{-/-}$*p53*$^{-/-}$ cells proliferated as rapidly and saturated at a similar density as *p53*$^{-/-}$ cells (Fig. 1a), and contained a significantly greater cycling population than *Ku80*$^{-/-}$ MEFs (Fig. 1b). Although the *Ku80*$^{-/-}$ proliferation defect was abrogated by the concomitant loss of *p53*, *Ku80*$^{-/-}$*p53*$^{-/-}$ MEFs were more sensitive to DNA damage induced by ionizing radiation than *p53*$^{-/-}$ or wild-type controls (Fig. 1c). After γ-irradiation,

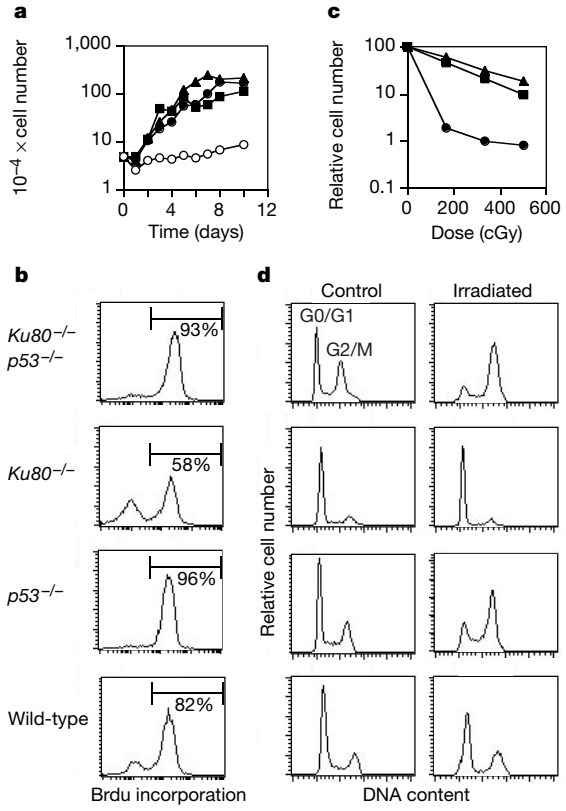

Figure 1 Growth characteristics of untreated and irradiated mouse embryo fibroblasts. **a**, Growth kinetics of *Ku80*$^{-/-}$ (open circles), *p53*$^{-/-}$ (filled triangles), *Ku80*$^{-/-}$*p53*$^{-/-}$ (filled circles) and wild-type (filled squares) MEFs. **b**, Incorporation of BrdU in MEF cultures after 16 h of continuous labelling. **c**, Radiation sensitivity of *Ku80*$^{-/-}$*p53*$^{-/-}$ (circles), *p53*$^{-/-}$ (triangles) and wild-type (squares) MEFs, plotted as the fraction of surviving cells relative to unirradiated samples of the same genotype. *Ku80*$^{-/-}$ MEFs exhibited a sevenfold decrease in cell count independent of the dose (83–600 cGy) owing to the premature senescence of unirradiated cultures, and the permanent arrest of the dividing population in response to γ-irradiation. **d**, DNA content histogram measured in untreated samples (control) and in cultures 24 h after treatment with 10 Gy of γ-radiation (Irradiated).

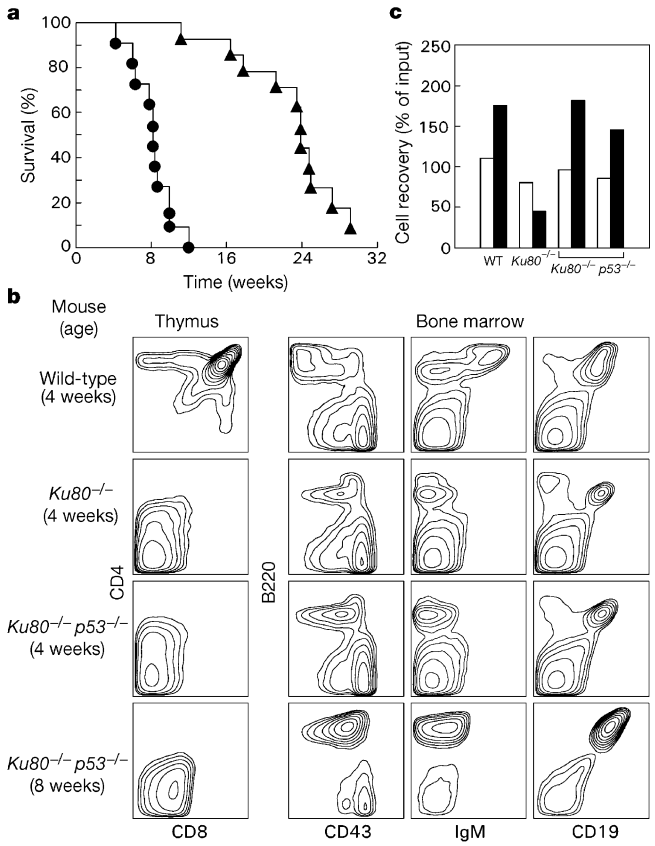

Figure 2 Analysis of lifespan and lymphocyte development. **a**, Kaplan–Meier analysis comparing mortality of *Ku80*$^{+/+}$*p53*$^{-/-}$ (triangles) and *Ku80*$^{-/-}$*p53*$^{-/-}$ (circles) mice as a function of time. The survival of *Ku80*$^{-/-}$*p53*$^{-/-}$ mice is statistically different from that of the *Ku80*$^{+/+}$*p53*$^{-/-}$ group; $P = 0.0001$. **b**, Flow cytometric analysis of thymocyte (left panel) and bone-marrow (right panels) suspensions obtained from wild-type, *Ku80*$^{-/-}$ and *Ku80*$^{-/-}$*p53*$^{-/-}$ mice. An 8-week-old *Ku80*$^{-/-}$*p53*$^{-/-}$ mouse, which had a B-cell lymphoma, is compared with a 4-week-old non-tumour-bearing *Ku80*$^{-/-}$*p53*$^{-/-}$ mouse, and with 4-week-old *Ku80*$^{-/-}$ and wild-type littermates. Data are representative of 10 wild-type, 6 *Ku80*$^{-/-}$, 5 non-tumour-bearing *Ku80*$^{-/-}$*p53*$^{-/-}$ mice 2–4 weeks old, and 12 *Ku80*$^{-/-}$*p53*$^{-/-}$ animals that had tumours. Average thymus cellularity was 5×10^5 in *Ku80*$^{-/-}$ mice, 10^6 in non-tumour-bearing *Ku80*$^{-/-}$*p53*$^{-/-}$ mice and 2×10^8 in wild-type controls. Average number of B220$^+$CD19$^+$ cells in bone marrow was 4.6×10^5 in *Ku80*$^{-/-}$ mice, 9.6×10^5 in non-tumour-bearing *Ku80*$^{-/-}$*p53*$^{-/-}$ mice and 2.8×10^6 for wild-type controls. The immuno-phenotypes of *Ku80*$^{+/+}$*p53*$^{-/-}$ and wild-type mice were similar (not shown). **c**, Survival of wild-type (WT) B220$^+$CD43$^+$IgM$^-$ pro-B cells, and *Ku80*$^{-/-}$*p53*$^{-/-}$ and *Ku80*$^{-/-}$ CD19$^+$ B cells after 1 d (open columns) and 3 d (filled columns) in culture, plotted relative to input cell number at day 0. Results from two independent *Ku80*$^{-/-}$*p53*$^{-/-}$ mice are plotted.

Ku80$^{-/-}$*p53*$^{-/-}$ MEFs initially accumulated in the G2/M phase of the cell cycle (Fig. 1d). Within 48–96 hours after irradiation, *Ku80*$^{-/-}$*p53*$^{-/-}$ MEFs lost their adherence to the tissue culture dish, exhibited extensive nuclear fragmentation and showed an increase in the number of cells with a DNA content less than that in G0/G1 (not shown). By contrast, *Ku80*$^{-/-}$ MEFs were arrested permanently in the G0/G1 and G2/M phases of the cell cycle in response to γ-irradiation[3] (Fig. 1d). Thus, p53 is required for early senescence in *Ku80*$^{-/-}$ fibroblasts, indicating that cell-cycle arrest in these cells is correlated with an accumulation of DNA damage (see below). The fact that a loss of p53 does not rescue the size of *Ku80*$^{-/-}$ mice indicates either that the dwarfism is unrelated to DNA damage or that *Ku80*$^{-/-}$*p53*$^{-/-}$ cells that sustain irreparable damage are eliminated by p53-independent mechanisms *in vivo*.

Although *Ku80*$^{-/-}$*p53*$^{-/-}$ mice developed normally, all (n = 11) such mice died within 12 weeks after birth (Fig. 2a) from disseminated lymphoma. Tumour cells expressed B-cell lineage-specific surface markers B220, CD19 and CD43, but were negative for IgM, indicating maturational arrest at the pro-B-cell stage of development (Fig. 2b; right panel, *Ku80*$^{-/-}$*p53*$^{-/-}$ 8 weeks). In contrast, *p53*$^{-/-}$ mice are predisposed to thymic lymphomas[11], which develop at a slower rate than *Ku80*$^{-/-}$*p53*$^{-/-}$ pro-B-cell lymphomas (Fig. 2a), and *Ku80*$^{-/-}$ mice only occasionally develop lymphoma[2] (only 1 out of 11 *Ku80*$^{-/-}$ mice developed T-cell lymphoma (Thy1.2$^+$, CD4$^+$, CD8$^+$) after seven months). We conclude that the loss of *p53* in the *Ku80* knockout background invariably results in the rapid onset of B-lineage tumours before the age at which T-lineage tumours occasionally arise in *Ku80*$^{-/-}$ mice.

The shift from T-cell to B-cell lymphomas in *Ku80*$^{-/-}$*p53*$^{-/-}$ mice was not accompanied by an obvious alteration in T- or B-lineage surface markers. *Ku80*$^{-/-}$*p53*$^{-/-}$ thymocytes resembled *Ku80*$^{-/-}$ thymocytes in that they developed no further than the CD4$^-$CD8$^-$ stage (Fig. 2b; left panel), whereas B cells remained arrested at the B220$^+$, CD19$^+$, CD43$^+$, IgM$^-$ pro-B-cell stage (Fig. 2b; right panel). However, the loss of *p53* had different effects on the survival of T-cell and B-cell precursors. Whereas both *Ku80*$^{-/-}$ pro-B and pro-T cells showed high susceptibility to apoptosis (as indicated by annexin staining; data not shown) and poor proliferation, loss of p53 from the double knockouts seemed to rescue *Ku80*$^{-/-}$ pro-B cells, but not pro-T cells (not shown), allowing normal proliferation *in vitro* (Fig. 2c). We conclude that p53 is required for the induction of apoptosis in B-lymphocyte but not T-lymphocyte precursors that harbour chromosome abnormalities induced by the loss of *Ku80*. This difference might in part explain the increased susceptibility of *Ku80*$^{-/-}$*p53*$^{-/-}$ mice to B-lineage malignancies.

The observation that *Ku80*$^{-/-}$*p53*$^{-/-}$ mice develop lymphomas at an accelerated rate suggests that Ku80 and p53 normally cooperate to limit the oncogenic potential of DSBs during assembly of the antigen receptor gene. Chromosome analysis by spectral karyotyping (SKY)[12] revealed karyotype heterogeneity within each *Ku80*$^{-/-}$*p53*$^{-/-}$ tumour (n = 4), exemplified by translocations and apparently random gains or losses of whole chromosomes (Fig. 3a). Metaphases from 20 identically treated *Rag2*$^{-/-}$ pro-B cells exhibited no detectable aberrations. All tumours contained a translocation of chromosome 12, on which the immunoglobulin heavy chain (IgH) is located (Fig. 3b; SKY). In three tumours (T2, T3 and T4) the partner was chromosome 15, whereas in the remaining tumour (T1) chromosome 3 was the fusion partner (Fig. 3b; SKY). The one *Ku80*$^{-/-}$ T-cell lymphoma that arose during the 7-month observation period exhibited a translocation that fused chromosomes 3 and 7 (not shown). Thus, both *Ku80*$^{-/-}$ and *Ku80*$^{-/-}$*p53*$^{-/-}$ mice develop lymphomas that exhibit chromosome translocations.

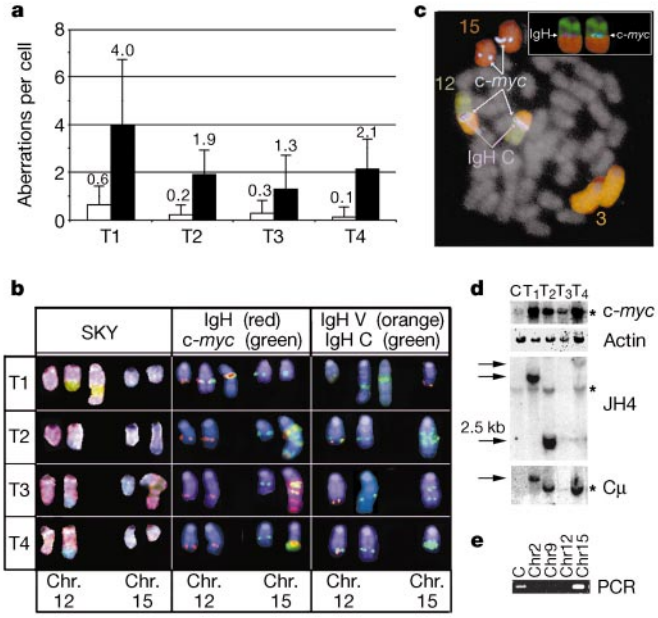

Figure 3 c-*myc* and IgH-associated rearrangements and amplifications in *Ku80*$^{-/-}$*p53*$^{-/-}$ tumours. **a**, Average number of translocations (other than those juxtaposing chromosomes 12 and 15), unshaded, or gains and loses of chromosomes, shaded, in *Ku80*$^{-/-}$*p53*$^{-/-}$ tumours (T1–T4). **b**, SKY analysis revealed translocations involving chromosomes (Chr.) 12 (pink) and 15 (blue) in *Ku80*$^{-/-}$*p53*$^{-/-}$ tumours 2–4 (T2–T4) and 12 and 3 (green) in T1. FISH with probes for IgH $C_{\gamma 1-\alpha}$ (red) and c-*myc* (green) reveal co-localization and co-amplification of these genes as well as signals on the normal chromosomes. Analysis with probes for IgH variable (orange) and constant (green) regions show co-localization on the normal chromosome 12. The absence of the variable region on the derivative 12 shows that this translocation disrupts the IgH locus. Chromosomes in the middle and right panels were identified by hybridization with painting probes (as in **c**) and are counterstained with 4,6-diamidino-2-phenylindole (DAPI; blue). **c**, Five-colour FISH analysis of a metaphase from tumour T1. The inset shows the localization of individual c-*myc* and IgH signals at the breakpoint between chromosomes 12 and 3. **d**, Southern blot analysis showing germline bands (stars) as well as rearrangments (arrows) and/or amplifications of c-*myc* and IgH. **e**, PCR amplification of tumour 2 breakpoint indicates that the JH1 fusion partner originated from chromosome 15. Abbreviations: C: Liver; T1–T4: *Ku80*$^{-/-}$*p53*$^{-/-}$ tumors 1–4.

Translocations between chromosomes 12 and 15 in *Ku80*$^{-/-}$*p53*$^{-/-}$ lymphomas resemble the translocations in mouse plasmacytomas and Burkitt's lymphomas that juxtapose the c-*myc* oncogene to the IgH locus[13]. Translocations involving the IgH locus, but not c-*myc*, have been reported in B-cell lymphomas arising from crosses between *SCID* (severe combined immunodeficiency) mice—which are defective in DNA-PKcs—and *p53*$^{-/-}$ mice[14]. We therefore performed fluorescence *in situ* hybridization (FISH) analysis to determine whether c-*myc* and IgH genes were translocated in *Ku80*$^{-/-}$*p53*$^{-/-}$ lymphomas. All *Ku80*$^{-/-}$*p53*$^{-/-}$ lymphomas showed co-localization of c-*myc* and IgH with an apparent amplification of both genes (Fig. 3b; IgH, c-*myc*). In the one *Ku80*$^{-/-}$*p53*$^{-/-}$ tumour that showed a 12:3 translocation, c-*myc* and IgH co-localized precisely at the breakpoint between chromosomes 12 and 3, indicating a three-way (12:15:3) translocation (Fig. 3c). Amplification of c-*myc* and IgH was confirmed by Southern blot analysis (Fig. 3d), and IgH locus rearrangements were found in all tumours (Fig. 3d). Furthermore, FISH analysis mapped the breakpoint on chromosome 12 to between the IgH variable cluster and constant region (Fig. 3b; IgH V, IgH C). We conclude that *Ku80*$^{-/-}$*p53*$^{-/-}$ lymphomas result from a specific set of chromosomal translocations and amplifications involving c-*myc* and IgH, and therefore differ from *SCIDxp53*$^{-/-}$ B-cell lymphomas[14]. DNA-PKcs-independent functions of Ku, as established in previous studies, might contribute to the cytogenetic differences in these tumours[3,15].

To determine the precise nature of the translocations in *Ku80*$^{-/-}$*p53*$^{-/-}$ lymphomas, we cloned the novel JH-hybridizing *Eco*RI fragment from one of the four tumours (Fig. 3d; T2). Sequence analysis revealed that the 2.5-kilobase (kb) fragment was a fusion of JH1 to a 173-base pair (bp) segment that bore no significant homologies to previously reported sequences. To determine the chromosomal origin of the 173-bp DNA fragment, FACS-sorted chromosomes were screened by PCR (Fig. 3e). Unfractionated liver DNA and purified chromosome 15 DNA showed a signal, whereas chromosomes 2, 9 and 12 were negative (Fig. 3e). Loss of the variable region on the der(12) chromosome and the proximity of the translocation to JH1 suggest that the translocation resulted from aberrant repair of DNA breaks produced in pro-B cells during V(D)J recombination.

One of the hallmarks of malignant transformation is genomic instability, which promotes a wide range of mutations, including chromosome deletions, gene amplifications, translocations and polyploidy[16]. To determine whether loss of *Ku80* results in chromosome instability, we karyotyped metaphases from passage-1 MEFs (Fig. 4). Whereas only 9% of metaphases from wild-type mice were karyotypically abnormal, we observed profound aberrations in the integrity of the *Ku80*$^{-/-}$ genome (Fig. 4a); 83% of *Ku80*$^{-/-}$ metaphases had breaks or translocations (Fig. 4a) and 15% displayed polyploidy (that is, 3*n*, 4*n* or 5*n* chromosome content, where 2*n* reflects a normal diploid complement). Although chromosome aberrations have been reported in primary dermal fibroblasts from *Ku80*$^{-/-}$, *Ku80*$^{+/-}$ and ligase IV$^{+/-}$ mice[17], we found no significant differences between *Ku80*$^{+/-}$ and wild-type MEFs. The pattern of damage in the *Ku80*$^{-/-}$ metaphases was further characterized by SKY, which showed chromatid breaks, acentric fragments, triradials, dicentrics, duplications and asymmetric exchanges (Fig. 4b). *Ku80*$^{-/-}$*p53*$^{-/-}$ MEFs were similar to *Ku80*$^{-/-}$, whereas *p53*$^{-/-}$ MEFs had slightly fewer aberrations (Fig. 4a). Thus, the absence of Ku80 precipitates genomic instability, which is not augmented by the additional loss of p53.

An apparently random gain or loss of chromosomes also occurred in 70% of *Ku80*$^{-/-}$ MEFs (not shown). Because aneuploidy has been associated with centrosome amplification in *BRCA1*$^{-/-}$ and *p53*$^{-/-}$ MEFs[18,19], we looked at these structures in early-passage MEFs. Our analysis of γ-tubulin structures revealed a similar centrosome amplification in both *Ku80*$^{-/-}$*p53*$^{-/-}$ and *p53*$^{-/-}$ MEFs. However, despite the numerical aberrations seen in *Ku80*$^{-/-}$ MEFs, centrosomes in these cells were indistinguishable from normal fibroblast controls (Fig. 4c; not shown). Thus, the acquisition of numerical chromosome aberrations in *Ku80*$^{-/-}$ MEFs occurs by a mechanism unrelated to centrosome amplification.

Unresolved signal ends in *Ku80*$^{-/-}$ lymphocytes might contribute to the development of translocations by acting as transposable elements[20,21]. Alternatively, gross chromosomal rearrangements in *Ku80*$^{-/-}$ mice might result from the absence of Ku-mediated tethering of broken ends, which normally facilitates their subsequent ligation[22,23]. Promiscuous chromosome fusions in the absence of Ku80 could either be accomplished by other components of the apparatus of the NHEJ pathway (that is, Ku70, DNA-PKcs, XRCC4 or Ligase IV) or involve alternative DNA repair pathways such as single-strand annealing or break-induced replication[24]. In either case, the finding that Ku80 suppresses gross genomic rearrangements places Ku80 in the class of caretaker genes, which include *ATM*, *BRCA1* and several proteins that function in homologous

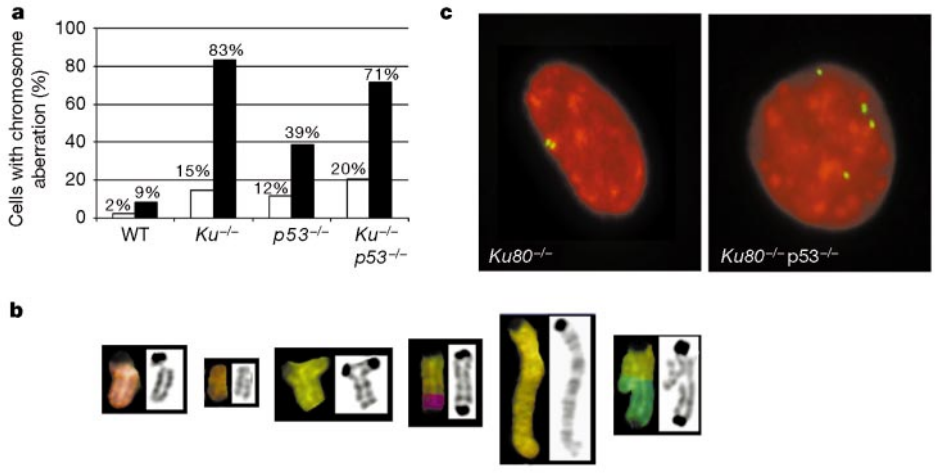

Figure 4 Chromosome aberrations in *Ku80*$^{-/-}$ and *Ku80*$^{-/-}$*p53*$^{-/-}$ MEFs. **a**, Percentage of cells with DNA breaks or translocations, shaded ($n = 35$), and polyploidy, unshaded ($n = 400$), observed in passage 1 MEFs. WT, wild type. **b**, Typical chromosome aberrations found in *Ku80*$^{-/-}$ MEFs. From left to right, chromatid break, acentric fragment, tri-radial, dicentric, duplication and an asymmetric exchange. **c**, γ-Tubulin staining for centrosomes (green) in *Ku80*$^{-/-}$ (left) and *Ku80*$^{-/-}$*p53*$^{-/-}$ (right) MEFs counterstained with propidium iodide (red).

recombination[1,25,26]. p53 provides an additional safeguard against the genomic instability inherent in Ku80-deficient cells by either arresting cell division (as in *Ku80*$^{-/-}$ MEFs) or triggering apoptosis (as in *Ku80*$^{-/-}$ B lymphocytes). Consistent with this model is the observation that the abrogation of both Ku80 caretaker and p53 gatekeeper functions markedly increases malignant transformation, especially in lymphocytes that undergo physiological DSBs during the course of V(D)J recombination. Whereas the phenotype of *Ku80*$^{-/-}$ mice is more severe than that of *DNA-PKcs*$^{-/-}$ mice, we would expect that other components of the NHEJ machinery (Ku70, XRCC4 and Ligase IV) also have an essential role in maintaining genomic stability. Thus, mutation of the NHEJ pathway components might facilitate the development of malignancy by increasing the frequency of chromosomal aberrations. □

Methods

Generation and screening of mice

Ku80 mutant mice were generated from *Ku80*$^{+/-}$ intercrosses and screened by polymerase chain reaction (PCR) as described[3]. *p53*$^{-/-}$ mice were obtained from Taconic Laboratories, and *p53* genotyping was performed as described[27,28]. Mice heterozygous for *Ku80* and *p53* were crossed to obtain progeny homozygous for both *Ku80*-null and *p53*-null alleles. To generate mouse embryo fibroblasts, *Ku80*$^{+/-}$*p53*$^{-/-}$ males were crossed with *Ku80*$^{+/-}$*p53*$^{+/-}$ females and embryos were isolated 13.5 days after plug formation[3].

Growth and irradiation assays

Passage-1 MEFs (10^5) were plated in duplicate six-well dishes and the medium was replaced daily. Individual dishes were treated with trypsin, counted and averaged. For continuous labelling experiments, 10^5 cells were plated with 50 μM bromodeoxyuridine (BrdU) and grown for 16 h. Cells were stained with fluorescein isothiocyanate (FITC)-conjugated anti-BrdU antibodies and propidium iodide (PI) in accordance with the manufacturer's specifications (Becton Dickinson). For radiation survival experiments, cells were exposed to graded doses of γ-rays, counted 4 d after irradiation, and normalized to the number of cells in unirradiated controls of the same genotype. Aliquots fixed at 24–96 h after irradiation were stained with PI for measurements of DNA content.

Spectral karyotyping, FISH and immunocytochemistry

MEFs from wild-type, *p53*$^{-/-}$, *Ku80*$^{-/-}$ and *Ku80*$^{-/-}$*p53*$^{-/-}$ mice were cultured in DMEM containing 10% fetal bovine serum (FBS). Suspensions of tumour cells derived from lymph node were grown in RPMI containing 10% FBS, 50 units ml^{-1} interleukin-7 (IL-7) (R&D Systems) and 20 units ml^{-1} IL-2 (Boehringer Mannheim). Tumour T1 was analysed after one passage in culture, whereas T2, T3 and T4 were primary tumours that were processed immediately for SKY, FISH and Southern blot analysis. MEFs and tumour cells were arrested at mitosis by treatment with Colcemid (Gibco/BRL) at 0.1 μg ml^{-1} for 0.5–3 h. Mitotic chromosome spreads were prepared by following standard procedures, and SKY analysis was performed as described[12]. For FISH analysis, metaphases were hybridized with BAC probes for the following regions: IgH constant region from $C_{\gamma 1}$ to 3′ of C_{α}, IgH variable region representing the distal end of the V cluster (VJ588), and c-*myc*. Flow-sorted single chromosomes were used for painting probes. Immunostaining of centrosomes with γ-tubulin antibodies was performed as described[29].

Flow cytometry

Single-cell suspensions from thymocytes, bone marrow, lymph node and tumours were stained for various lineage-specific surface markers as described[3]. The following monoclonal antibodies (PharMingen) were used in various two-colour combinations: phycoerythrin (PE)-conjugated anti-CD4 (clone RM4-5), FITC-conjugated anti-CD8a (clone 53-6.7), FITC-conjugated anti-T-cell antigen receptor (clone H57-597), PE-conjugated anti-B220 (clone RA3-6B2), FITC-conjugated anti-CD19 (clone 1D3), FITC-conjugated anti-IgM (clone II/41), FITC-conjugated anti-CD43 (clone S7) and PE-conjugated Thy1.2 (clone 53-2.1). At least 100,000 data points were collected on a modified immunocytometry systems FACSSTAR Plus using CellQuest software (Becton Dickinson).

Lymphocyte purification and culture

Bone marrow B cells from mutant and wild-type mice were enriched by positive selection with MACS mouse CD19 microbeads (Miltenyi Biotech). Wild-type B cells were further sorted into B220^{+}CD43^{+}CD25^{-}IgM^{-} pro-B cells. Pro-B cells were co-cultured for 3 d with irradiated S17 stromal cells and mouse rIL-7 (10 ng ml^{-1}). Wild-type CD4^{-}CD8^{-} T-cell precursors were enriched by negative selection with magnetic beads coated with anti-mouse CD4 and anti-mouse CD8 (Dynal). Apoptosis and viability of B and T cells were analysed with PE-Annexin (Pharmingen) and staining with PI.

Southern blot analysis and digestion–circularization PCR

Genomic DNA (10 μg) from *Ku80*$^{-/-}$*p53*$^{-/-}$ tumours was digested with *Eco*RI. Southern blots were sequentially hybridized to ^{32}P-labelled probes for c-*myc* and mouse actin cDNA; a duplicate blot was prepared and sequentially hybridized with a 1.1-kb JH4 and a 900-bp Cμ genomic fragment. For digestion–circularization PCR[30], 2 μg of genomic DNA was digested with *Eco*RI and ligated under dilute conditions that promote self-ligation[30]. Primers JH4F (5′-CTTCCCCAAATAGCCTTGCC-3′) and JH4R (5′-CCCACCAAACCG AAAGTCCA-3′) were used to amplify the 2.5-kb product by using the Expand High Fidelity PCR System (Boehringer). The amplified product was cloned into PCR-XL-TOPO (Invitrogen) and individual clones were isolated for sequencing. PCR primers PTK2F (5′-TGAGTTTCTTGGGTGTGGGC-3′) and PTK2R (5′-GCATAGGATTC GGCGTAGA-3′), derived from the 173-bp sequence fused to JH1, were used to screen 10 ng of DNA derived from liver and flow-sorted mouse chromosomes 2, 9, 12 and 15.

Received 4 January; accepted 22 February 2000.

1. Kinzler, K. W. & Vogelstein, B. Gatekeepers and caretakers. *Nature* **386,** 761–763 (1997).
2. Vogel, H., Lim, D. S., Karsenty, G., Finegold, M. & Hasty, P. Deletion of Ku86 causes early onset of senescence in mice. *Proc. Natl Acad. Sci. USA* **96,** 10770–10775 (1999).
3. Nussenzweig, A. *et al.* Requirement for Ku80 in growth and immunoglobulin V(D)J recombination. *Nature* **382,** 551–555 (1996).
4. Zhu, C., Bogue, M. A., Lim, D. S., Hasty, P. & Roth, D. B. Ku86-deficient mice exhibit severe combined immunodeficiency and defective processing of V(D)J recombination intermediates. *Cell* **86,** 379–389 (1996).
5. Ouyang, H. *et al.* Ku70 is required for DNA repair but not for T cell antigen receptor gene recombination *in vivo*. *J. Exp. Med.* **186,** 921–929 (1997).
6. Gu, Y. *et al.* Growth retardation and leaky SCID phenotype of Ku70-deficient mice. *Immunity* **7,** 367–376 (1997).
7. Gao, Y. *et al.* A critical role for DNA end-joining proteins in both lymphogenesis and neurogenesis. *Cell* **95,** 891–902 (1998).
8. Frank, K. M. *et al.* Late embryonic lethality and impaired V(D)J recombination in mice lacking DNA ligase IV. *Nature* **396,** 173–177 (1998).
9. Barnes, D. E., Stamp, G., Rosewell, I., Denzel, A. & Lindahl, T. Targeted disruption of the gene encoding DNA ligase IV leads to lethality in embryonic mice. *Curr. Biol.* **8,** 1395–1398 (1998).
10. Levine, A. J. p53, the cellular gatekeeper for growth and division. *Cell* **88,** 323–331 (1997).
11. Jacks, T. *et al.* Tumor spectrum analysis in p53-mutant mice. *Curr. Biol.* **4,** 1–7 (1994).
12. Liyanage, M. *et al.* Multicolour spectral karyotyping of mouse chromosomes. *Nature Genet.* **14,** 312–315 (1996).
13. Taub, R. *et al.* Translocation of the c-*myc* gene into the immunoglobulin heavy chain locus in human Burkitt lymphoma and murine plasmacytoma cells. *Proc. Natl Acad. Sci. USA* **79,** 7837–7841 (1982).
14. Vanasse, G. J. *et al.* Genetic pathway to recurrent chromsome translocations in murine lymphoma involves V(D)J recombinase. *J. Clin. Invest.* **103,** 1669–1675 (1999).
15. Gao, Y. *et al.* A targeted DNA-PKcs-null mutation reveals DNA-PK-independent functions for KU in V(D)J recombination. *Immunity* **9,** 367–376 (1998).
16. Lengauer, C., Kinzler, K. W. & Vogelstein, B. Genetic instabilities in human cancers. *Nature* **396,** 643–649 (1998).
17. Karanjawala, Z. E., Grawunder, U., Hsieh, C. L. & Lieber, M. R. The nonhomologous DNA end joining pathway is important for chromosome stability in primary fibroblasts. *Curr. Biol.* **9,** 1501–1504 (1999).
18. Fukasawa, K., Choi, T., Kuriyama, R., Rulong, S. & Vande Woude, G. F. Abnormal centrosome amplification in the absence of p53. *Science* **271,** 1744–1747 (1996).
19. Xu, X. *et al.* Centrosome amplification and a defective G2-M cell cycle checkpoint induce genetic instability in BRCA1 exon 11 isoform-deficient cells. *Mol. Cell* **3,** 389–395 (1999).
20. Agrawal, A., Eastman, Q. M. & Schatz, D. G. Transposition mediated by RAG1 and RAG2 and its implications for the evolution of the immune system. *Nature* **394,** 744–751 (1998).
21. Hiom, K., Melek, M. & Gellert, M. DNA transposition by the Rag1 and Rag2 proteins: a possible source of oncogenic translocations. *Cell* **94,** 463–470 (1998).
22. Ramsden, D. A. & Gellert, M. Ku protein stimulates DNA end joining by mammalian DNA ligases: a direct role for Ku in repair of DNA double-strand breaks. *EMBO J* **17,** 609–614 (1998).
23. Smith, G. C. M. & Jackson, S. P. The DNA-dependent protein kinase. *Genes Dev.* **13,** 916–934 (1999).
24. Chen, C., Umezu, K. & Kolodner, R. D. Chromosomal rearrangements occur in *S. cerevisiae* rfa1 mutator mutants due to mutagenic lesions processed by double-strand-break repair. *Mol. Cell* **2,** 9–22 (1998).
25. Moynahan, M. E., Chiu, J. W., Koller, B. H. & Jasin, M. Brca1 controls homology-directed DNA repair. *Mol. Cell* **4,** 511–518 (1999).
26. Johnson, R. D., Liu, N. & Jasin, M. Mammalian XRCC2 promotes the repair of DNA double-strand breaks by homologous recombination. *Nature* **401,** 397–399 (1999).
27. Timme, T. L. & Thompson, T. C. Rapid allelotype analysis of p53 knockout mice. *Biotechniques* **17,** 462–463 (1994).
28. Donehower, L. A. *et al.* Mice deficient for p53 are developmentally normal but susceptible to spontaneous tumours. *Nature* **356,** 215–221 (1992).
29. Ghadimi, B. M. *et al.* Centrosome amplification and instability occurs exclusively in aneuploid, but not in diploid colorectal cancer cell lines, and correlates with numerical chromosomal aberrations. *Genes Chromosomes Cancer* **27,** 183–190 (2000).
30. Chu, C. C., Paul, W. E. & Max, E. E. Quantitation of immunoglobulin μ-γ1 heavy chain switch region recombination by a digestion–circularization polymerase chain reaction method. *Proc. Natl Acad. Sci. USA* **89,** 6978–6982 (1992).

Acknowledgements

We thank A. Singer, R. Hodes, A. Bhandoola, E. Besmer and S. Sharrow for comments on the manuscript and helpful discussions; K. Huppi, B. Malynn and R. Riblet for probes; and D. Liewehr, S. Steinberg and T. Brotz for assistance. M.C.N. is an investigator of the Howard Hughes Medical Institute. A.N. was supported in part by an award from the Arthritis Foundation.

Correspondence and requests for materials should be addressed to A.N. (e-mail: andre_nussenzweig@nih.gov).